

Predicting the structure and energy of a grain boundary in germanium

This article has been downloaded from IOPscience. Please scroll down to see the full text article.

1989 J. Phys.: Condens. Matter 1 327

(<http://iopscience.iop.org/0953-8984/1/2/001>)

View [the table of contents for this issue](#), or go to the [journal homepage](#) for more

Download details:

IP Address: 171.66.16.89

The article was downloaded on 10/05/2010 at 15:54

Please note that [terms and conditions apply](#).

Predicting the structure and energy of a grain boundary in germanium

E Tarnow[†], P D Bristowe[†], J D Joannopoulos[†] and M C Payne[‡]

[†] Massachusetts Institute of Technology, Cambridge, MA 02139, USA

[‡] Cavendish Laboratory, Madingley Road, Cambridge CB3 0HE, UK

Received 14 June 1988, in final form 23 August 1988

Abstract. An *ab initio* molecular dynamics simulated quenching approach is used to study the properties of a (001) twist grain boundary in the $\Sigma = 5$ system in germanium. Interfacial total energies are mapped out over the entire range of possible relative in-plane translation states of the boundary. The analysis leads to predictions of the equilibrium translation state, the geometric structure, effective local volume and formation energy associated with this internal interface.

Recent experimental advances in the microscopic characterisation of grain boundaries in solids have stimulated considerable theoretical interest in providing realistic structural models for these important planar defects. High-resolution electron microscopy [1] and x-ray diffraction [2] techniques can now determine atomic positions in the core of the grain boundary to an accuracy of better than 0.2 Å. The preferred theoretical approach for reproducing or predicting this level of structural information requires a formal quantum mechanical treatment of the total energy of the grain boundary environment that correctly takes into account the unrestricted relaxation of the ions and the corresponding redistribution of electron charge density. However, the general structural complexity of grain boundaries makes this a formidable task. As a consequence, the limited number of quantum mechanical calculations performed to date have, by necessity, imposed a variety of geometrical constraints and physical approximations [3–8]. The purpose of the present paper is to demonstrate that a first-principles calculation of the structure and energy of a short-period grain boundary in germanium that avoid many of these restrictions can be performed. In particular, an *ab initio* total energy formalism (see for example [9]), based on a molecular dynamics simulated quenching method [10, 11], is employed to map out inter-granular interaction energies over the entire range of possible relative translation states in the plane of the boundary. The analysis leads to predictions of the equilibrium translation state, microscopic geometric structure, effective local volume, and grain boundary formation energy.

The specific boundary we consider is a high-angle (001) twist boundary in the diamond cubic lattice and is part of the $\Sigma = 5$ system (Σ refers to the inverse density of coincidence sites). As described elsewhere [12–14], the two-point basis of the diamond lattice results in the generation of two distinct coincidence site patterns (or dichromatic complexes)

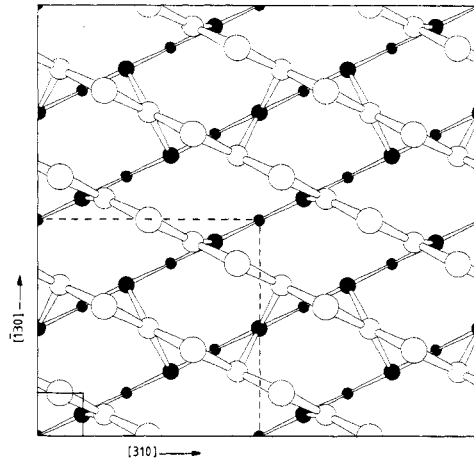


Figure 1. Atomic positions in planes normal to the $[001]$ direction for two layers above (open circles) and below (full circles) an unrelaxed $\Sigma 5^*$ twist grain boundary in germanium. The CSL unit cell is indicated by broken lines and the smaller DSC cell is indicated by full lines. There is no relative translation of the upper and lower layers.

for any given density of coincidence sites. Thus, in the $\Sigma = 5$ system, rotations about $[001]$ through $(0, 0, 0)$ by 36.9° or -53.1° result in different atomic structures. Since the two structures are not related by a translation in the plane of the boundary, we choose, for simplicity, to distinguish them with the notation $\Sigma 5 (36.9^\circ)$ and $\Sigma 5^* (-53.1^\circ)$. As seen later, this distinction is useful in discussing the different structural domains that may occur in the $\Sigma = 5$ system. In the present paper, we focus attention on the $\Sigma 5^*$ boundary and its associated translation states in the (001) grain boundary plane.

Figure 1 illustrates the atomic positions of two layers on either side of the unrelaxed $\Sigma 5^*$ boundary. The atoms are connected by bonds if their relative distance is less than 15% of the bulk bond length (previous calculations [15] of bond charge density have shown this cut-off to be realistic.) The coincidence site lattice (CSL) unit cell is outlined by broken lines in the lower left quadrant, and the axis of rotation, which is normal to the figure, passes through the atom at the centre of the cell. The CSL unit-cell edge vectors are $\frac{1}{2}a[310]$ (horizontal direction) and $\frac{1}{2}a[\bar{1}30]$ (vertical direction), where a is the lattice parameter. The small cell located in the lower left corner of the figure is the DSC (displacement shift complete) unit cell. The DSC lattice has the property that translations of one crystal grain with respect to the other by a DSC unit-cell vector conserve the boundary structure. The DSC unit-cell edge vectors are $\frac{1}{10}a[310]$ and $\frac{1}{10}a[\bar{1}30]$. The irreducible zone of the DSC unit cell is a quarter of the original cell and defines all unique translation states of the boundary. Any translations outside this zone will give configurations that are related to the ones inside the zone by symmetry. One remarkable property of this zone is its size—only 1% of the area of the CSL. Also translations along $[310]$ within the zone are not equivalent to translations along $[\bar{1}30]$. Furthermore, it can be shown that translations to the four corners of the irreducible zone produce unrelaxed structures which have higher symmetry than any other general translation within the zone and are, therefore, predicted to have symmetry-dictated extrema in energy. These translations are 0 , $\frac{1}{20}a[310]$, $\frac{1}{20}a[\bar{1}30]$ and $\frac{1}{10}a[210]$.

Previous theoretical [3, 5] and experimental [16] studies of semiconductor grain

boundaries have shown that in-plane translations between neighbouring grains can lead to low-energy structures. Our own preliminary calculations [3] on the $\Sigma 5^*$ boundary, where we examined only two distinct translation states, showed that a shift of $\frac{1}{10}a[210]$ away from coincidence could lower the boundary energy by 33%. It is clear that any thorough calculation of the true equilibrium state of a boundary must include not only the local relaxations of the boundary atoms, but also the unrestricted relaxation of the translation state. To satisfy this requirement, we have employed the following relaxation strategy. As a first approximation, we calculate the unrelaxed total energy of the boundary in nine different in-plane translation states which are distributed on a square grid within the irreducible zone of the DSC unit cell. In the second step, local atomic relaxations are allowed in the core region of each boundary translation state but the relative position of the two adjoining grains is kept fixed (changes in volume are, however, allowed). Lastly, we take the lowest-energy structure found from this procedure and lift the constraint on the translation state; we thus obtain by further relaxation the equilibrium configuration. In this way, most of the phase space of the grain boundary can be accessed. We note, however, that the following assumptions remain implicit in our model: the fundamental structural unit of the boundary is still defined by the primitive CSL vectors (i.e., there are no larger units caused by reconstructions); the average atomic density remains that of the bulk (i.e., there are no structural vacancies or interstitials); and the boundary width is confined to two atomic layers on either side of the interface. Since reconstructions, which are common on surfaces (see, for example [17]), have been reported at only one grain boundary [18], and since experiments suggest that boundary widths are extremely narrow [19], our assumptions seem to be justified.

In calculating the total energy of each configuration, we use six standard approximations. These are: the pseudopotential approximation where we use an *ab initio* local Starkloff–Joannopoulos potential for Ge [9] (the parameters we used were $\lambda_c = 18$ au and $r_c = 1.05$ au⁻¹ and they reproduce the atomic wavefunctions and eigenvalues to within 2%); the local density approximation using the Perdew–Zunger parametrisation for the exchange correlation potential [20]; the special *k*-point method [21]; the supercell approximation, including a finite number of basis states; and a finite Fourier transform grid consisting of $20 \times 20 \times 36$ grid points. We used plane waves with kinetic energies less than 125 eV or about 70 plane waves per atom. The two *k*-points used were $(\frac{1}{4}, \frac{1}{4}, 0)$ and $(-\frac{1}{4}, \frac{1}{4}, 0)$, and increasing to five *k*-points made the total energy change by less than 0.05 eV per boundary. All of these approximations were tested and it was found that the results should be reliable to within 0.5 eV for the boundary energy, to within 0.05 Å per unit area for the local volume change, and to within 6% of the irreducible DSC cell for the position of the translation state. The supercell contains twelve (004) layers, each with five atoms, separated into two six-layer crystal slabs rotated relative to each other by -53.1° . The slabs are $8.8 \text{ \AA} \times 8.8 \text{ \AA}$ in cross section (the CSL periodicity). All atoms in the supercell are allowed to relax except for those in the central two layers of each crystal slab which are confined to their bulk positions. In addition, the distances between all layers in the grain boundary region are allowed to relax except the distance between the two central bulk-like layers of each slab. (An estimate of the error arising from this supercell approximation can be obtained by also allowing the atoms in the third, ‘bulk-like’, layer of the slab to relax. We performed this test for our final low-energy structure and the results were as follows: the grain boundary energy changed by less than 0.2 eV, the positions of the third-layer atoms changed by less than 0.04 Å, the second-layer atoms by less than 0.01 Å and, finally, the atoms in the layer closest to the boundary relaxed by less than 0.005 Å.)

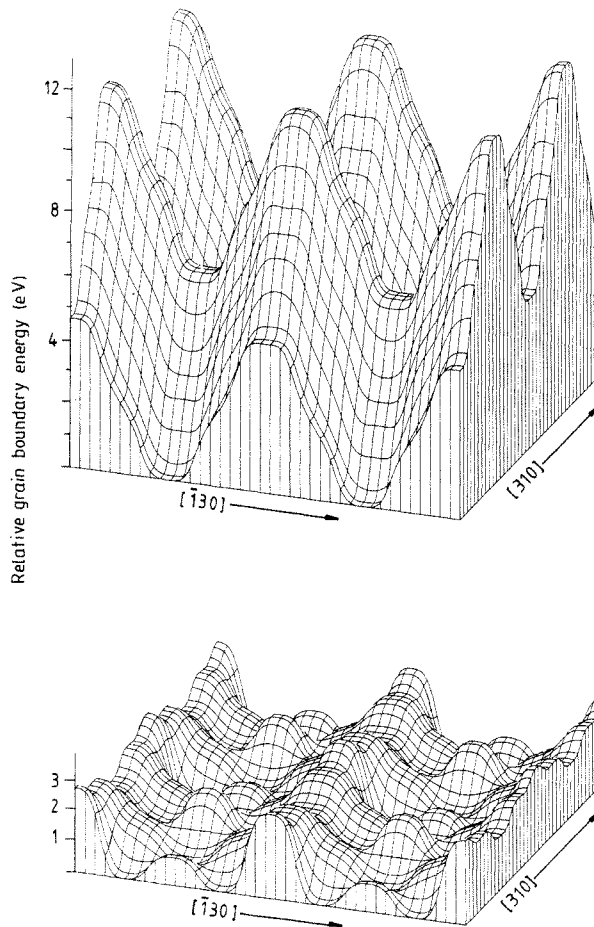


Figure 2. The energy translation surface for the $\Sigma 5^*$ boundary before and after relaxation (upper and lower panels). Each surface covers four DSC unit cells and the boundary energies are normalised to the minima in each case. The minima in the unrelaxed surface are located at $\frac{1}{2}a[\bar{1}30]$ and the minima in the relaxed surface are located at $\frac{1}{4}a[\bar{1}30]$.

The positions of the atoms within the unit cell are found by a rapid quenching of their velocities using the molecular dynamics method. During this quenching, the initial structures relax to local minimum-energy states. The atoms are moved along the Hellmann–Feynman [22] forces about $4 \text{ m}\text{\AA}$ per iteration. About 200 iterations of the ionic degrees of freedom are needed before the boundary energy has converged to within 0.05 eV and the Hellmann–Feynman forces are less than about 0.1 eV \AA^{-1} .

The results from calculating the unrelaxed total energy at each of the nine translation states within the irreducible zone of the DSC cell are presented in the top panel of figure 2. The translation states fall on a square grid whose spacing is a quarter of the DSC periodicity, so the energy translation surface shown in figure 2 represents an interpolation between the calculated points. Also, for clarity, the surface is drawn over four DSC unit cells. It is seen immediately that the extrema in unrelaxed energy are located at the four structures with the highest symmetry. The minimum is at $\frac{1}{2}a[\bar{1}30]$, the maximum at $\frac{1}{2}a[310]$, and the $\frac{1}{4}a[210]$ and $\frac{1}{4}a[310]$ states are saddle points. The topology of this

interfacial total energy map is easily explained by comparing the unrelaxed geometric structures of each of the translation states. We find that the maximum-energy-translation state corresponds to a distribution of atoms in adjacent layers where some atoms are forced to be close together in unfavourable bonding positions. On the other hand, the minimum-energy-translation state corresponds to the most balanced distribution of atoms creating the best opportunity for bond formation across the interface. Does the energy surface have the same topology when local atomic relaxations and volume changes are allowed? The bottom panel of figure 2 shows the total-energy surface after these additional structural degrees of freedom are relaxed. The lack of correspondence between the two surfaces is striking. The relaxed energy range is only 3 eV compared with 11 eV for the rigid layers. There are now three local maxima rather than one, and the original maximum has become a saddle point and the original minimum has become a local maximum. The lowest-energy state is now located at the position $\frac{1}{40}a[\bar{1}30]$. All the translation states exhibit a positive local volume change per unit area (compared with the bulk) of 0.1–0.3 Å. The boundary with maximum unrelaxed energy (where some atoms were close together) has the largest volume change and the boundary with minimum unrelaxed energy has the smallest volume change. Examination of the nine relaxed structures shows that several of them, grouped in pairs or triples, are nearly identical. This is very interesting because it indicates that there are small regions of the irreducible zone that favour one, and only one, distinct structure. Of particular interest is the region surrounding the relaxed energy minimum. The configuration common to this region is characterised by the presence of three fold and five fold-coordinated atoms, [110] dimers, and ring structures containing five or more atoms. The boundary energy for some of these similar structures is quite different, however. This is attributed to strain interactions between atoms in the core boundary region and those in the more bulk-like upper layers.

In the final step of our relaxation process, the lowest-energy configuration with translation state $\frac{1}{40}a[\bar{1}30]$ is taken and the constraint on the relative position of the fixed outer layers is lifted. In this calculation, the fixed outer layers are effectively allowed to ‘float’ over the core region of the boundary until they experience a zero net force. At the same time, the boundary atoms may rearrange if they prefer. The result is that the relative translation of the grains shifts to $\frac{1}{20}a[\bar{1}30]$ but that the connectivity of the core boundary atoms remains virtually unchanged! The total energy of the configuration drops by 42% (3.8 to 2.2 eV), which is apparently due to a relaxation of the strain energy between the second layer from the boundary and the outer bulk atoms. The bond angles and bond lengths between these layers become very close to the bulk values indicating that the final structure is virtually strain free. It is clear, therefore, that the low-energy structure described above, which was characteristic of the region surrounding the $\frac{1}{40}a[\bar{1}30]$ translation state, is very stable with respect to small shifts of the adjoining grains. However, overall, it prefers to be embedded between two grains that are translated by $\frac{1}{20}a[\bar{1}30]$ with respect to one another. Figure 3 illustrates the final equilibrium $\Sigma 5^*$ boundary structure obtained in our study. The same criterion for bonding atoms is used as in figure 1. We see that four of the ten atoms closest to the boundary have fourfold coordination with small bond angle distortions, two of them are fourfold coordinated with large bond angle distortions, two of them are fivefold coordinated and the remaining two are threefold coordinated. There are no rings present consisting of less than five atoms and there are two dimer-like bonds present per unit CSL cell. Note that the structure in figure 3 does not possess the symmetry that one might naively expect for $\frac{1}{20}a[\bar{1}30]$. We believe this is a result of a symmetry-breaking arising from a ‘Jahn–

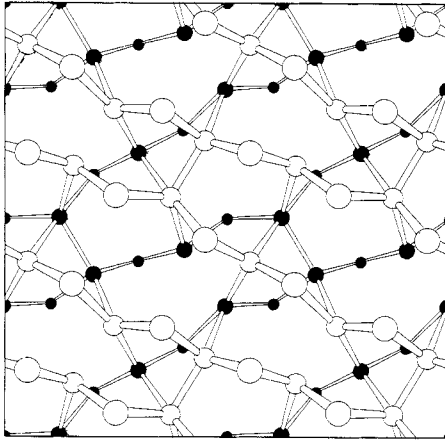


Figure 3. The lowest-energy $\Sigma 5^*$ boundary structure after full relaxation. The translation state is $\frac{1}{20}a[\bar{1}30]$. Note the threefold- and fivefold-coordinated atoms and $[110]$ dimers.

Teller' type of distortion. In a symmetric structure, all (save two) atoms per unit cell adjacent to the boundary would be either dimerised or undimerised. In either case, this leads to energetically unfavourable configurations of atoms and the system prefers to compromise with a mixture of dimerised and undimerised atoms. The local volume change at the boundary is positive and equal to 0.1 \AA per unit area, and the grain boundary energy is 482 mJ m^{-2} .

As a check to determine the possible existence of boundary structures with even lower energies, the following test calculations were performed. All the differently connected structures obtained from the initial relaxations were re-relaxed using the $\frac{1}{20}a[\bar{1}30]$ translation state. No structures of lower energy were found.

Experimentally, the structure and energy of the $\Sigma 5^*$ boundary have not been measured. However, if it were possible to fabricate precisely a -53.1° (001) twist boundary in germanium, our results indicate that it should have the translation state, coordination, local expansion and energy described above. Unfortunately, in an actual twist boundary in the $\Sigma = 5$ system, deviations in the angle of rotation and location of the boundary plane will result in the presence of dislocations and additional structural domains [13]. As described earlier, two distinct CSL patterns are crystallographically possible, which we have labelled $\Sigma 5^* (-53.1^\circ)$ and $\Sigma 5 (36.9^\circ)$. These two geometries are related by an out-of-plane translation equal to $\frac{1}{20}a[315]$. Thus, $\Sigma 5^*$ may be transformed into $\Sigma 5$ by an operation that involves the removal or insertion of a (004) plane normal to the boundary. Since, experimentally, it would be difficult to control the location of the boundary plane (due, for example, to (001) surface steps if the boundary is formed by sintering) then the actual boundary may be composed of domains of both $\Sigma 5^*$ and $\Sigma 5$ structure. The coexistence of such domains has already been observed in a $\Sigma = 5$ (310) system in germanium [13]. Since the present paper has focused on the $\Sigma 5^*$ structure, further calculations on the $\Sigma 5$ counterpart are required to determine the overall structural characteristics of the $\Sigma = 5$ system. A final experimental complication would be the presence of non-primitive structural units (supercells) at the boundary in analogy to the (2×1) reconstruction that forms on the (001) surface. Whether or not such boundary reconstructions are energetically favourable is also to be the subject of future calculations.

Acknowledgments

This work was supported in part by the US Air Force Office of Scientific Research Contract No 87-0098, by the National Science Foundation Grant No DMR 84-18718 and by the Science and Engineering Research Council Grant No GR/E/25948. PDB wishes to acknowledge the financial assistance and hospitality of the TCM group at the Cavendish Laboratory where, during his visit, this study was initiated.

References

- [1] Bourret A 1985 *J. Physique Coll.* **46** C4 27
- [2] Fitzsimmons M R and Sass S L 1988 *Acta Metall.* **36** 3103
- [3] Payne M C, Bristowe P D and Joannopoulos J D 1987 *Phys. Rev. Lett.* **58** 1348
- [4] Thomson R E and Chadi D J 1984 *Phys. Rev. B* **29** 889
- [5] DiVincenzo D P, Alerhand O L, Schluter M and Wilkins J W 1986 *Phys. Rev. Lett.* **56** 1925
- [6] Chou M Y, Cohen M L and Louie S G 1985 *Phys. Rev. B* **32** 7979
Zhang S B, Cohen M L and Louie S G 1986 *Phys. Rev. B* **34** 768
- [7] Mauger A, Bourgoin J C, Allan G, Lannoo M, Bourret A and Billard L 1987 *Phys. Rev. B* **35** 1267
- [8] Smith J R and Ferrante J 1986 *Phys. Rev. B* **34** 2238
- [9] Joannopoulos J D 1985 *Physics of Disordered Materials* ed. D Adler, H Fritzsche and S R Ovshinsky (New York: Plenum) p 19
- [10] Car R and Parrinello M 1985 *Phys. Rev. Lett.* **55** 2471
- [11] Payne M C, Joannopoulos J D, Allan D C, Teter M P and Vanderbilt D H 1986 *Phys. Rev. Lett.* **56** 2656
- [12] Pond R C 1983 *Microscopy of Semiconducting Materials 1983* (Inst. Phys. Conf. Ser. 67) p 59
- [13] Bacmann J J, Silvestre G, Petit M and Bollmann W 1981 *Phil. Mag. A* **43** 189
- [14] Pond R C and Vlachavas D S 1983 *Proc. R. Soc. A* **386** 95
- [15] Payne M C, Bristowe P D and Joannopoulos J D 1989 *J. Physique Coll.* at press
- [16] Bourret A and Bacmann J J 1985 *Surf. Sci.* **162** 495
- [17] Needels M, Payne M C and Joannopoulos J D 1987 *Phys. Rev. Lett.* **58** 1765
- [18] Bourret A and Bacmann J J 1986 *Trans. Japan. Inst. Met. Suppl.* **27** 125
- [19] Vaudin M D, Lamarre P A, Schmuckle F and Sass S L 1986 *Phil. Mag. A* **54** 21
- [20] Perdew P and Zunger A 1981 *Phys. Rev. B* **23** 5048
- [21] Monkhorst H J and Pack J D 1976 *Phys. Rev. B* **16** 5188
- [22] Hellmann H 1937 *Einführung in die Quarter Theorie* (Leipzig: Deuticke) p 285
Feynman R P 1939 *Phys. Rev.* **56** 340